
Analytical, Optimal, and Sparse Optimal Control of Traveling Wave Solutions to Reaction-Diffusion Systems

Christopher Ryll¹, Jakob Löber², Steffen Martens², Harald Engel², and Fredi Tröltzsch¹

¹ Technische Universität Berlin, Institut für Mathematik, 10623 Berlin, Germany

² Technische Universität Berlin, Institut für Theoretische Physik, 10623 Berlin, Germany

Abstract. This work deals with the position control of selected patterns in reaction-diffusion systems. Exemplarily, the Schlögl and FitzHugh-Nagumo model are discussed using three different approaches. First, an analytical solution is proposed. Second, the standard optimal control procedure is applied. The third approach extends standard optimal control to so-called sparse optimal control that results in very localized control signals and allows the analysis of second order optimality conditions.

Introduction

Beside the well-known Turing patterns, reaction-diffusion (RD) systems possess a rich variety of self-organized spatio-temporal wave patterns including propagating fronts, solitary excitation pulses, and periodic pulse trains in one-dimensional media. These patterns are “building blocks” of wave patterns like target patterns, wave segments, and spiral waves in two as well as scroll waves in three spatial dimensions, respectively. Another important class of RD patterns are stationary, breathing, and moving localized spots [1–7].

Several control strategies have been developed for purposeful manipulation of wave dynamics as the application of closed-loop or feedback-mediated control loops with and without delays [8–11] and open-loop control that includes external spatio-temporal forcing [10, 12–14], optimal control [15–17], and control by imposed geometric constraints and heterogeneities on the medium [18, 19]. While feedback-mediated control relies on continuously monitoring of the system’s state, open-loop control is based in general on a detailed knowledge of the system’s dynamics and its parameters.

For example, different feedback control loops have been realized in experiments with the photosensitive Belousov-Zhabotinsky (BZ) reaction using

feedback signals obtained from wave activity measured at one or several detector points, along detector lines, or in a spatially extended control domain including global feedback control [8,9,20]. Varying the excitability of the light-sensitive BZ medium by changing the globally applied light intensity forces a spiral wave tip to describe a wide range of hypocycloidal and epicycloidal trajectories [21,22]. Moreover, feedback-mediated control loops has been applied successfully in order to stabilize unstable patterns in experiments, such as unstable traveling wave segments and spots [11]. Two feedback loops were used to guide unstable wave segments in the BZ reaction along pre-given trajectories [23]. An open loop control was successfully deployed in dragging traveling chemical pulses of adsorbed CO during heterogeneous catalysis on platinum single crystal surfaces [24]. In these experiments, the pulse velocity was controlled by a laser beam creating a movable localized temperature heterogeneity on an addressable catalyst surface, resulting in a V-shaped pattern [25]. Dragging a one-dimensional chemical front or phase interface to a new position by anchoring it to a movable parameter heterogeneity, was studied theoretically in [26,27].

Recently, an open-loop control for controlling the position of traveling waves over time according to a prescribed *protocol of movement* $\phi(t)$ was proposed that simultaneously preserves the wave profile [28]. Although position control is realized by external spatio-temporal forcing (i.e., belongs to open-loop control), quite importantly no detailed knowledge about the reaction dynamics as well as the system parameters is needed. We have already demonstrated the ability of position control to accelerate or decelerate traveling fronts and pulses in one spatial dimension for a variety of RD models [29,30]. In particular, we found that the analytically derived control function is close to a numerically obtained optimal control solution. A similar approach allows to control the two-dimensional shape of traveling wave solutions. Control signals that realize a desired wave shape are determined analytically from nonlinear evolution equation for isoconcentration lines as the perturbed nonlinear phase diffusion equation or the perturbed linear eikonal equation [31]. In the work at hand, we compare our analytic approach for position control with optimal trajectory tracking of RD patterns in more detail. In particular, we quantify the difference between an analytical solution and a numerically obtained result to optimal control, thereby determining the conditions under which the numerical result approaches the analytical result. This establishes a basis for using analytical solutions to speed up numerical computations of optimal control and serve as a consistency check for numerical algorithms.

We consider the following structure of a linearly controlled RD system

$$\partial_t \mathbf{u}(\mathbf{x}, t) - \mathcal{D} \Delta \mathbf{u}(\mathbf{x}, t) + \mathbf{R}(\mathbf{u}(\mathbf{x}, t)) = \mathcal{B} \mathbf{f}(\mathbf{x}, t). \quad (1)$$

Here, $\mathbf{u}(\mathbf{x}, t) = (u_1(\mathbf{x}, t), \dots, u_n(\mathbf{x}, t))^T$ is a vector of n state components in a bounded or unbounded spatial domain $\Omega \subset \mathbb{R}^N$ of dimension $N \in \{1, 2, 3\}$, \mathcal{D}

is an $n \times n$ matrix of diffusion coefficients which is implied to be diagonal for an isotropic medium, $\mathbf{D} = \text{diag}(D_1, \dots, D_n)$, Δ represents the N -dimensional Laplacian operator, and \mathbf{R} denotes the vector of the n in general nonlinear reaction kinetics. The vector of control signals $\mathbf{f}(\mathbf{x}, t) = (f_1(\mathbf{x}, t), \dots, f_m(\mathbf{x}, t))^T$ acts in time and space. Equation (1) must be supplemented with an initial condition $\mathbf{u}(\mathbf{x}, t_0) = \mathbf{u}_0(\mathbf{x})$ and appropriate boundary conditions. A common choice are no-flux boundary conditions at the boundary $\Sigma = \partial\Omega \times (0, T)$, $\partial_n \mathbf{u}(\mathbf{x}, t) = \mathbf{0}$, where $\partial_n \mathbf{u}$ denotes the component-wise spatial derivative in the direction normal to the boundary $\Gamma = \partial\Omega$.

Typically, the number m of independent control signals in Eq. (1) is smaller than the number n of state components. We call such a system an *underactuated* system. The $n \times m$ matrix \mathbf{B} determines which state components are directly affected by the control signals. If $m = n$ and the matrix \mathbf{B} is regular, it is called a *fully actuated* system.

Our main goal is to identify a control \mathbf{f} such that the state \mathbf{u} follows a desired spatio-temporal trajectory \mathbf{u}_d , also called desired distribution, as closely as possible everywhere in space Ω and for all times $0 \leq t \leq T$. We can measure the distance between the actual solution \mathbf{u} of the controlled RD system Eq. (1) and the desired trajectory \mathbf{u}_d up to the terminal time T with the non-negative functional

$$J(\mathbf{u}) = \|\mathbf{u} - \mathbf{u}_d\|_{L^2(Q)}^2, \quad (2)$$

where $\|\cdot\|_{L^2(Q)}^2$ is the L^2 -norm,

$$\|\mathbf{h}\|_{L^2(Q)}^2 = \int_0^T \int_{\Omega} d\mathbf{x} dt \{ \mathbf{h}(x, t)^2 \}, \quad (3)$$

in the space-time-cylinder $Q := \Omega \times (0, T)$. The functional Eq. (2) reaches its smallest possible value, $J = 0$, if and only if the controlled state \mathbf{u} equals the desired trajectory almost everywhere in time and space. In many cases, the desired trajectory \mathbf{u}_d cannot be exactly realized by the control, but one might be able to find a control which enforces the state \mathbf{u} to follow \mathbf{u}_d as closely as possible as measured by J . A control function \mathbf{f} is *optimal* if it realizes a state \mathbf{u} which minimizes J . The method of optimal control views J as a constrained functional subject to \mathbf{u} satisfying the controlled RD system Eq. (1). Often, the minimum of the objective functional J does not exist. Hence, additional (inequality) constraints such as bounds for the control function must be introduced to ensure the existence, cf. Ref. [32]. Alternatively, in one and two spatial dimensions, it is also possible to do so by adding a so-called Tikhonov-regularization term to Eq. (2) which is quadratic in the control,

$$J(\mathbf{u}, \mathbf{f}) = \|\mathbf{u} - \mathbf{u}_d\|_{L^2(Q)}^2 + \nu \|\mathbf{f}\|_{L^2(Q)}^2. \quad (4)$$

The L^2 -norm of the control \mathbf{f} is weighted by a very small coefficient $\nu > 0$. This parameter might be interpreted as a control cost to achieve a certain state \mathbf{u} . Since the control \mathbf{f} does not come for free, there is a “price” to pay. Yet, its presence causes the state to be further away from the desired trajectories or final states than in the case of $\nu = 0$. Mathematically, ν serves as a regularization parameter that stabilizes the numerical computations. Moreover, it guarantees the existence of an *optimal control* f , denoted by \bar{f} , in one and two spatial dimensions if the bounds on the control signal are missing.

In addition to the weighted L^2 -norm of the control, other terms can be added to the functional Eq. (4). An interesting choice is the weighted L^1 -norm such that the functional reads

$$J(\mathbf{u}, \mathbf{f}) = \|\mathbf{u} - \mathbf{u}_d\|_{L^2(Q)}^2 + \nu \|\mathbf{f}\|_{L^2(Q)}^2 + \kappa \|\mathbf{f}\|_{L^1(Q)}, \quad (5)$$

with $\kappa > 0$. For appropriate values of $\kappa > 0$, the corresponding optimal control becomes sparse, i.e., it only acts in some localized regions of the space-time-cylinder while it vanishes identically everywhere else. Therefore, it is also called *sparse control* or *sparse optimal control* in literature, see Refs. [33–36]. In some sense, we can interpret the areas with non-zero optimal control signals as most efficient areas to manipulate the RD patterns in order to behave in the desired way expressed by \mathbf{u}_d . Further, the weighted L^1 -norm enables the investigation of the behavior of solutions for a Tikhonov-regularization parameter ν tending to zero. This allows to draw conclusions about the approximation of solutions to unregularized problems by regularized ones.

This work is organized as follows: In Sect. 1, we present an analytical approach for the control of the position of RD patterns. These analytical expressions solve the problem of minimizing the unregularized ($\nu = 0$) functional Eq. (2) and might provide an appropriate initial guess for optimal control. In Section 2, we state explicitly the optimal control problem for traveling waves solutions to the Schlögl or Nagumo model and the FitzHugh-Nagumo model. Both are well-known models to describe traveling fronts and pulses in one spatial dimension, solitary spots and spiral waves in two spatial dimensions, and scroll waves in three spatial dimensions [4, 10, 37]. We compare the analytical solutions with numerically obtained regularized optimal control solutions for the position control of a traveling front solution in the Schlögl model in Section 2.3. In particular, we demonstrate the quality of the analytical solution to the numerical obtained results from the optimal control problem for decreasing values ν . They agree almost perfectly if ν is chosen sufficiently small. Section 3 discusses sparse optimal control in detail and presents numerical examples obtained with the FitzHugh-Nagumo system. Finally, we conclude our findings in Sect. 4.

1 Analytical approach

Below, we sketch the idea of analytical position control of RD patterns proposed previously in Refs. [28, 29]. For simplicity, we consider a single-component RD system of the form

$$\partial_t u(x, t) - D\Delta u(x, t) + R(u(x, t)) = f(x, t), \quad (6)$$

in one spatial dimension $x \in \mathbb{R}^1$. Hence, the state u as well as the control signal f are scalar functions and the system Eq. (6) is fully actuated. Exploiting the relation between control f and state u Eq. (6), one simply inserts the desired trajectory u_d for u in Eq. (6) and obtains for the control

$$f(x, t) = \partial_t u_d(x, t) - \Delta u_d(x, t) + R(u_d(x, t)). \quad (7)$$

Obviously, the desired trajectory u_d must be sufficiently smooth to evaluate $\partial_t u_d$ and Δu_d everywhere in space-time-cylinder Q . We call the desired trajectory u_d exactly realizable if the controlled state u equals u_d everywhere in Q , i.e., $u(x, t) = u_d(x, t)$. This can only be true if two more conditions are satisfied: First, the initial condition for the controlled state must coincide with the initial state of the desired trajectory, i.e., $u(x, t_0) = u_d(x, t_0)$, and, secondly, all boundary conditions obeyed by u have to be obeyed by u_d as well. If these assumptions are satisfied, the control solution f , Eq. (7), realizes the desired trajectory exactly, $u(x, t) = u_d(x, t)$. Therefore, the corresponding unregularized functional J , Eq. (2), vanishes identically. The control f is certainly a control which minimizes the unregularized functional J and, in particular, it is *optimal*. A more rigorous evaluation based on the necessary optimality condition for the minimization of the regularized functional, Eq. (4), leads to the same conclusion [38].

Generalizing the procedure to multi-component RD systems Eq. (1), the expression for the control reads

$$\mathbf{f}(x, t) = \mathbf{B}^{-1}(\partial_t \mathbf{u}_d(x, t) - \mathcal{D}\Delta \mathbf{u}_d(x, t) + \mathbf{R}(\mathbf{u}_d(x, t))). \quad (8)$$

Once more, the initial and boundary conditions for the desired trajectory have to comply with the initial and boundary conditions of the state. Clearly, the inverse of \mathbf{B} exists if and only if \mathbf{B} is a regular square matrix, i.e., the system must be fully actuated. We emphasize the generality of the result. Apart from mild conditions on the differentiability of the desired distributions \mathbf{u}_d , (8) yields a simple expression for the control signal of arbitrary \mathbf{u}_d .

Next, we consider exemplarily the position control of traveling waves (TW) in one spatial dimension. Traveling waves are solutions to the uncontrolled RD system, Eq. (1) with $\mathbf{f} = \mathbf{0}$, characterized by a wave profile $\mathbf{u}(x, t) = \mathbf{U}_c(x - ct)$. In the co-moving frame of reference, $\xi = x - ct$, the wave profile \mathbf{U}_c is stationary and satisfies the following differential equation,

$$\mathcal{D}\mathbf{U}_c''(\xi) + c\mathbf{U}_c'(\xi) - \mathbf{R}(\mathbf{U}_c(\xi)) = \mathbf{0}, \quad \xi \in \Omega \subset \mathbb{R}, \quad (9)$$

The prime denotes differentiation with respect to ξ and c is the velocity of the TW. We emphasize that stationary solutions with $c = 0$ are also considered as traveling waves. The ODE for the wave profile, Eq. (9), can exhibit one or more homogeneous steady states. Typically, the wave profile \mathbf{U}_c approaches either two different steady states or the same steady state for $\xi \rightarrow \pm\infty$. This fact can be used to classify traveling wave profiles. Front profiles connect different steady states for $\xi \rightarrow \pm\infty$ and are found to be heteroclinic orbits of Eq. (9), while pulse profiles join the same steady state and are found to be homoclinic orbits. Furthermore, all TW solutions are localized in the sense that their spatial derivatives of any order $m \geq 1$ decay to zero, $\lim_{\xi \rightarrow \pm\infty} \partial_\xi^m \mathbf{U}_c(\xi) = 0$.

We emphasize that the proposed spatio-temporal control $f(x, t)$ attempts to control the position of a traveling wave over time t according to a prescribed *protocol of movement* $\phi(t)$ while preserving simultaneously the uncontrolled wave profile \mathbf{U}_c . Consequently, the desired trajectory reads $\mathbf{u}_d(x, t) = \mathbf{U}_c(x - \phi(t))$. The initial condition for the state is $\mathbf{u}_0(x, t_0) = \mathbf{U}_c(x - x_0)$ which fixes the initial value of the protocol of motion as $\phi(t_0) = x_0$. Moreover, there are boundary conditions to be satisfied at $\xi = \pm\infty$. Then, the control solution Eq. (8) becomes

$$\mathbf{f}(x, t) = \mathcal{B}^{-1}(-\dot{\phi}(t)\mathbf{U}'_c(x - \phi(t)) - \mathcal{D}\mathbf{U}''_c(x - \phi(t)) + \mathbf{R}(\mathbf{U}_c(x - \phi(t)))). \quad (10)$$

Using Eq. (9) to eliminate the non-linear reaction kinetics \mathbf{R} , finally we obtain the following analytical expression for the spatio-temporal control

$$\mathbf{f}(x, t) = (c - \dot{\phi}(t))\mathcal{B}^{-1}\mathbf{U}'_c(x - \phi(t)) =: \mathbf{f}_{\text{an}}. \quad (11)$$

Remarkably, any reference to the reaction function \mathbf{R} drops out from the expression for the control. This is of great advantage for applications because the underlying nonlinear reaction kinetics \mathbf{R} is often unknown. If the propagation velocity c is known and the uncontrolled wave profile can be measured with sufficient accuracy to calculate the Goldstone mode \mathbf{U}'_c , the method is applicable.

A general problem of position control, being an open loop control, is its possible inherent instability against perturbations of the initial conditions [29]. However, for protocol velocities $\dot{\phi}(t)$ close to the uncontrolled velocity c , $\dot{\phi} \sim c$, the control solution Eq. (11) enforces a wave profile which is relatively close to the uncontrolled TW profile \mathbf{U}_c . Since the uncontrolled TW is presumed to be stable, the controlled TW might benefit from that and thus a stable open loop control is expected. This expectation is confirmed numerically for a variety of controlled RD systems [28], and also analytically [29].

Despite the advantages of our analytical solution stated above, there are limits for it as well. The restriction to fully actuated systems, i.e., systems for which \mathcal{B}^{-1} exists, is not always practical. In experiments with RD systems, the number of state components is usually much larger than one while the number of control signals is often restricted to one or two. Thus, the question arises

if the approach can be extended to underactuated systems with a number of independent control signals smaller than the number of state components. This is indeed the case but entails additional assumptions about the desired trajectory. In the context of position control of TWs, it leads to a control which is not able to preserve the TW profile for all state components, see Ref. [28]. The general case will be discussed in a forthcoming thesis [38] and is not part of this paper.

Moreover, it is often necessary to impose inequality constraints in form of upper and lower bounds on the control in applications. For example, the intensity of a heat source deployed as the control is bounded by technical reasons. Even worse, if the control is the temperature itself it is impossible to attain negative values. Since the control signal \mathbf{f}_{an} is proportional to the slope of the controlled wave profile \mathbf{U}'_c , the magnitude of the applied control may locally attain non-realizable values. In our analytic approach, Eq. (11), no bounds for the control signal are imposed. The control signal \mathbf{f}_{an} is optimal only in case of a vanishing Tikhonov-regularization parameter $\nu = 0$, cf. Eq. (4). Moreover, target distributions \mathbf{u}_d which do not comply with initial as well as boundary conditions or are non-smooth might be desired. These cannot be controlled by the analytical solution but optimal control can deal with many of these complications.

2 Optimal Control

In the following, we recall the optimal control problem and sketch the most important analytical results to provide the optimality system.

2.1 The Control Problem

For simplicity, we state the optimal control problem explicitly the FitzHugh-Nagumo system [39, 40]. The FitzHugh-Nagumo system is a two-component model $\mathbf{u} = (u, v)^T$ for an activator u and an inhibitor v ,

$$\begin{aligned} \partial_t u(\mathbf{x}, t) - \Delta u(\mathbf{x}, t) + R(u(\mathbf{x}, t)) + \alpha v(\mathbf{x}, t) &= f(\mathbf{x}, t), \\ \partial_t v(\mathbf{x}, t) + \beta v(\mathbf{x}, t) - \gamma u(\mathbf{x}, t) + \delta &= 0, \end{aligned} \quad (12)$$

in a bounded Lipschitz-domain $\Omega \subset \mathbb{R}^N$ of dimension $1 \leq N \leq 3$. Since the single-component control f appears solely on the right-hand side of the first equation, this system is *underactuated*. Allowing a control in the second equation is fairly analogous. The kinetic parameters α , β , γ , and δ are real numbers with $\beta \geq 0$. Moreover, the reaction kinetics is given by the nonlinear function $R(u) = u(u - a)(u - 1)$ for $0 \leq a \leq 1$. We emphasize that the equation for the activator u decouples from the equation for the inhibitor v for $\alpha = 0$, cf. Eqs. (12), resulting in the Schlögl model [1, 41]. Further, we assume homogeneous Neumann-boundary conditions for the activator u and

$u(\mathbf{x}, 0) = u_0(\mathbf{x})$, $v(\mathbf{x}, 0) = v_0(\mathbf{x})$ are given initial states belonging to $L^\infty(\Omega)$, i.e., they are bounded.

The aim of our control problem is the tracking of desired state functions $\mathbf{u}_d = (u_d, v_d)^T$ in the space-time cylinder Q and to reach terminal states $\mathbf{u}_T = (u_T, v_T)^T$ at final time T . In contrast to the analytic approach Eq. (11), these desired functions are neither assumed to be smooth nor compatible with the given initial data or boundary conditions. For simplicity, we assume their boundedness, i.e., $(u_d, v_d)^T \in (L^\infty(Q))^2$ and $(u_T, v_T)^T \in (L^\infty(\Omega))^2$. The goal of reaching the desired states is expressed as the minimization of the objective functional

$$\begin{aligned} J(u, v, f) = & \frac{1}{2} \left(c_T^U \|u(\cdot, T) - u_T\|_{L^2(\Omega)}^2 + c_T^V \|v(\cdot, T) - v_T\|_{L^2(\Omega)}^2 \right) \\ & + \frac{1}{2} \left(c_d^U \|u - u_d\|_{L^2(Q)}^2 + c_d^V \|v - v_d\|_{L^2(Q)}^2 \right) + \frac{\nu}{2} \|f\|_{L^2(Q)}^2. \end{aligned} \quad (13)$$

This functional is slightly more general than the one given by Eq. (2) because it takes account of the terminal states as well. We emphasize that the given non-negative coefficients c_d^U , c_d^V , c_T^U , and c_T^V can also be chosen as functions depending on space and time. In some applications, this turned out to be very useful [42]. In all cases, we assume that the parameter ν is non-negative and in particular positive ($\nu > 0$) in numerical computations.

Moreover, the control functions can be taken out of the set of admissible controls

$$\mathcal{F}_{\text{ad}} = \{f \in L^\infty(Q) : u_a \leq f(\mathbf{x}, t) \leq u_b, \text{ for } (\mathbf{x}, t) \in Q\}. \quad (14)$$

The bounds $u_a < u_b$ model the technical capacities for generating controls. If this is not important, they can be set to $u_a = -\infty$ and/or $u_b = \infty$.

Under the previous assumptions, the controlled RD equations (12) have a unique weak solution denoted by $(u_f, v_f)^T$ for a given control f . This solution is bounded, i.e., $u_f, v_f \in L^\infty(Q)$. If the initial data $(u_0, v_0)^T$ are continuous, then u_f and v_f are continuous on $\bar{\Omega} \times [0, T]$ with $\bar{\Omega} = \Omega \cup \partial\Omega$. Moreover, the control-to-state mapping $G := f \mapsto (u_f, v_f)^T$ is twice continuously (Fréchet-) differentiable. A proof can be found in Ref. [42, Theorem 2.1, Corollary 2.1, and Theorem 2.2]. Expressed in terms of the solution $(u_f, v_f)^T$, the value of the objective functional depends only on f , $J(u, v, f) = J(u_f, v_f, f) =: F(f)$, and the optimal control problem can be formulated in a condensed form as

$$(P) \quad \text{Min } F(f), \quad f \in \mathcal{F}_{\text{ad}}. \quad (15)$$

In contrast to the analytical approach presented in Sect. 1, the numerical and theoretical treatment of (P) is easier for a positive regularization-parameter $\nu > 0$. This parameter might be interpreted as a control cost to achieve a certain state \mathbf{u} . Although a finite value $\nu > 0$ is often necessary for the analysis of the problem on the one hand and increases the stability of numerical

computations of an optimal control on the other hand, the case $\nu = 0$ is of special interest. Naturally, the solution \mathbf{u} for $\nu = 0$ - if it exists - is the closest (in the $L^2(Q)$ -sense) to the desired trajectory \mathbf{u}_d among all optimal solutions associated with any $\nu \geq 0$. Therefore, it can be seen as the limit of the realizability of a certain desired trajectory \mathbf{u}_d .

Mathematically, ν serves as a regularization parameter that guarantees the existence of an *optimal control* f , denoted by \bar{f} , in one and two spatial dimensions if the bounds u_a, u_b on the control signal are missing, i.e., $u_a = -\infty, u_b = \infty$. If $N \geq 3$ and one of the desired states is not exactly realizable, the problem (P) is not solvable with unconstrained controls. For numerical simulations, ν is chosen to lie in the range 10^{-8} to 10^{-3} . Despite this small value, it nevertheless has an effect on states and control as well as on the value of the objective functional.

Referring to [42, Theorem 3.1], we know that the control problem (P) has at least one (optimal) solution \bar{f} for all $\nu \geq 0$. To determine this solution numerically, we need the first and second-order derivatives of the objective function F . Since the mapping $f \mapsto (u, v)^T$ is twice continuously differentiable, so is $F : L^p(Q) \rightarrow \mathbb{R}$. To compute the derivatives at the current control f , we have to proceed as follows:

First, we have to compute $(u_f, v_f)^T$ as solution to the system Eqs. (12). Next, we insert $(u_f, v_f)^T$ into the so-called adjoint system, a linearized version of Eqs. (12), to obtain the adjoint state $(\varphi_f, \psi_f)^T$, cf. Ref. [42, §3.2]. Then, the first derivative $F'(f)$ in the direction $h \in L^p(Q)$ can be computed as follows

$$F'(f)h = \int\int_{0,\Omega}^T d\mathbf{x} dt \{(\varphi_f + \nu f)h\}. \quad (16)$$

This first derivative is used in numerical methods of gradient type. Higher order methods of Newton type need also the second derivative $F''(f)$. It reads, in a single direction $h \in L^p(Q)$,

$$\begin{aligned} F''(f)h^2 &= \int_{\Omega} d\mathbf{x} \{c_T^U \eta_h(\mathbf{x}, T)^2 + c_T^V \zeta_h(\mathbf{x}, T)^2\} \\ &+ \int\int_{0,\Omega}^T d\mathbf{x} dt \{[c_d^U - R''(u_f)\varphi_f]\eta_h^2 + c_d^V \zeta_h^2\} + \nu \int\int_{0,\Omega}^T d\mathbf{x} dt \{h^2\}. \end{aligned} \quad (17)$$

In this expression, $(\eta_h, \zeta_h) := G'(u_f)h$ denotes the solution of a linearized FitzHugh-Nagumo system, cf. Ref. [42, Theorem 2.2]. Such linearized systems appear naturally in Newton type methods.

2.2 First-Order Optimality Conditions

We emphasize that the control problem (P) is not convex. Although the objective function $J(u, v, f)$ is convex, the nonlinearity of the mapping $f \mapsto$

$(u_f, v_f)^T$ will lead to a non-convex function, F . Therefore, (P) is a problem of non-convex optimization, possibly leading to several local minima instead of a single global minimum.

As in standard calculus, we invoke first-order necessary optimality conditions to find a (locally) optimal control \bar{f} . In the case of unconstrained control, i.e., $\mathcal{F}_{\text{ad}} := L^p(Q)$, the first derivative of F must be zero, $F'(\bar{f}) = 0$. Computationally, this condition is better expressed in the equivalent form

$$F'(\bar{f})f = \int_0^T \int_{\Omega} d\mathbf{x} dt \{(\bar{\varphi} + \nu \bar{f})f\} = 0, \text{ for all } f \in L^p(Q), \quad (18)$$

where $\bar{\varphi}$ denotes the first component of the adjoint state associated with \bar{f} . If \bar{f} is not locally optimal, one finds a descent direction d such that $F'(\bar{f})d < 0$. This is used for methods of gradient type.

If the restrictions \mathcal{F}_{ad} are given by Eq. (14), then Eq. (18) does not hold true in general. Instead, the variational inequality

$$F'(\bar{f})(f - \bar{f}) = \int_0^T \int_{\Omega} d\mathbf{x} dt \{(\bar{\varphi} + \nu \bar{f})(f - \bar{f})\} \geq 0, \forall f \in \mathcal{F}_{\text{ad}} \cap U(\bar{f}), \quad (19)$$

must be fulfilled. Here $U(\bar{f}) \subset L^p(Q)$ denotes a neighborhood of \bar{f} . Roughly speaking, it says that in a local minimum we cannot find an admissible direction of descent. A gradient method would stop in such a point. A pointwise discussion of Eq. (19) leads to the following identity:

$$\bar{f}(\mathbf{x}, t) = \text{Proj}_{[u_a, u_b]} \left(-\frac{1}{\nu} [\bar{\varphi}(\mathbf{x}, t)] \right), \text{ for } \nu > 0. \quad (20)$$

Here, $\text{Proj}_{[u_a, u_b]}(x) = \min\{\max\{u_a, x\}, u_b\}$ denotes the projection to the interval $[a, b]$. We remark that numerical solutions can be obtained by solving the system Eq. (12) and the adjoint system such that the last identity Eq. (20) is fulfilled.

2.3 Example 1: Analytical and Optimal Position Control

In 1972, Schlögl discussed the auto-catalytic trimolecular RD scheme [1, 41] as a prototype of a non-equilibrium first order phase transition. The reaction kinetics R for the chemical with concentration $u(x, t)$ is cubic and can be casted into this dimensional form $R(u) = u(u - a)(u - 1)$. The associated controlled RD equation reads

$$\partial_t u - \Delta u + u(u - a)(u - 1) = f(x, t), \quad 0 < a < 1.$$

A linear stability analysis of the controlled system reveals that $u = 0$ and $u = 1$ represents stable spatially homogeneous steady states (HSS) while $u = a$ is an

unstable homogeneous steady state. In an infinite one-dimensional domain, the Schlögl model possesses a stable traveling wave solution whose profile is given by

$$U_c(\xi) = 1 / \left(1 + \exp \left(\xi / \sqrt{2} \right) \right), \quad (21)$$

in the co-moving frame of reference $\xi = x - ct$. This front solution establishes a transition between two stable HSS for $\xi \rightarrow \pm\infty$ and travels with a velocity $c = (1 - 2a) / \sqrt{2}$ from the left to the right.

As an example, we aim to accelerate a traveling front according to the following protocol of motion

$$\phi(t) = -10 + ct + \frac{10 - 1/\sqrt{2}}{200} t^2, \quad (22)$$

while keeping the front profile as close as possible to the uncontrolled one. In other words, our desired trajectory reads $u_d(x, t) = U_c(x - \phi(t))$, and consequently the initial condition of both the controlled and the desired trajectory is $u(x, 0) = u_0(x) = U_c(x + 10)$. In our numerics, we set $T = 20$ for the terminal time T , $\Omega = (-25, 25)$ for the spatial domain, and the threshold parameter is kept fixed at $a = 9/20$. Additionally, we choose the terminal state to be equal to the desired trajectory, $u_T(x) = u_d(x, T)$, and set the remaining weighting coefficients to unity, $c_d^U = c_T^U = 1$, in the optimal control problem. The space-time plot of the desired trajectory u_d is presented in Fig. 1a for the protocol of motion $\phi(t)$ as given in Eq. (22).

Below, we compare the numerically obtained solution to the optimal control problem (P) with the analytical solution from Sect. 1 for the Schlögl model. The Schlögl model arises from Eq. (12) by setting $\alpha = 0$ and ignoring the inhibitor variable v . Consequently, all weighting coefficients associated with the inhibitor trajectory are set to zero, $c_d^V = c_T^V = 0$, in the functional J , Eq. (13).

In Fig. 1b, we depict the solution for the analytic position control f_{an} , valid solely for a vanishing Tikhonov regularization parameter $\nu = 0$. Obviously, the numerically obtained optimal control \bar{f} , see Fig. 1c, does not differ visually from the analytic one. Both are located at the front position where the slope is maximal, $\mathbf{u}_d = 0.5$ (dashed line in Fig. 1b), and their magnitudes grow proportional to $\dot{\phi}(t)$. For comparison, we compute additionally the distance between analytical and optimal control signal $\|\bar{f} - f_{\text{an}}\|_2$ in the sense of $L^2(Q)$, Eq. (3), and normalized it by the size of the space-time-cylinder $|Q| = T |\Omega|$

$$\|h\|_2 := \frac{1}{|Q|} \|h\|_{L^2(Q)}. \quad (23)$$

In the top row of Table 1, we display the distance $\|\bar{f} - f_{\text{an}}\|_2$ as a function of the regularization parameter ν . Even for a large value of $\nu = 1$, the distance is less than 5×10^{-4} and thus small. For decreasing values of ν , the difference

lessens as well and saturates quickly at $\simeq 8 \times 10^{-6}$. The saturation of the distance arises due to discretization errors of the numerical solution as well as due to the fact that optimal controls were computed in a bounded interval $\Omega = (-25, 25)$ with homogeneous Neumann-boundary conditions. Strictly speaking, the selected desired trajectory requires either an infinite domain or non-homogeneous boundary conditions to be an exactly realizable trajectory [31].

Another interesting question is how close the controlled state u_f approaches the desired trajectory u_d . The bottom row of Table 1 shows the distance between the optimal controlled state trajectory u_f and the desired trajectory for different values of $\nu > 0$. Similarly, the difference decreases with decreasing values of ν . Note that the value for the difference does not saturate and becomes much smaller than the distance between the controls $\|\bar{f} - f_{\text{an}}\|_2$. No discretization errors arise because a discretized version of the desired trajectory is used as the target distribution. Nevertheless, errors arise because neither the initial desired state or the desired trajectory nor the final desired state perfectly obey the Neumann-boundary conditions in the finite simulation domain. This can lead to an optimal control signal exhibiting bumps close to the boundary. However, since the derivative of the traveling front solution Eq. (21) decays exponentially for large $|x|$, the violation of boundary conditions is negligible as long as the protocol of motion is designed such that it keeps the traveling front sufficiently far away from any boundary. In our example, the maximal violation of the Neumann-boundary condition is in the range 1.75×10^{-5} .

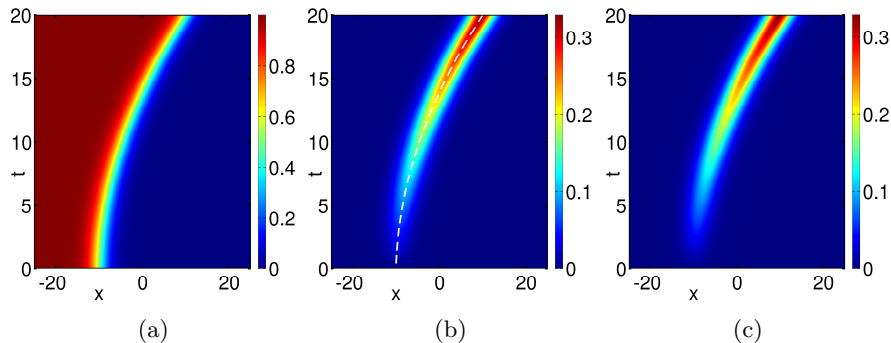


Fig. 1. (a) Space-time plot of the desired trajectory $u_d(x, t) = U_c(x - \phi(t))$ with the protocol of motion $\phi(t)$ as given in Eq. (22), (b) analytic position control $f_{\text{an}}(x, t)$, Eq. (11), and (c) numerically obtained optimal control \bar{f} for Tikhonov regularization parameter $\nu = 10^{-5}$ are presented. The magnitude of the control signal is color-coded. The dashed line represents $\phi(t)$ in the center panel. The remaining parameter values are $a = 9/20$, $T = 20$, and $c_d^U = c_T^U = 1$.

Table 1. The distance $\|\bar{f} - f_{\text{an}}\|_2$ between the analytically obtained control signal f_{an} , valid solely for $\nu = 0$, and the numerically obtained optimal control \bar{f} for finite $\nu > 0$ shows a decrease with lessen value of ν (top row). Similarly, the optimal controlled state trajectory u_f comes closer to the desired trajectory u_d , measured by $\|u_f - u_d\|_2$, for a smaller value of ν (bottom row).

ν	1	E-1	E-2	E-3	E-4	E-5	E-6
$\ \bar{f} - f_{\text{an}}\ _2$	4.57E-4	1.14E-4	2.50E-5	1.01E-5	8.40E-6	8.30E-6	8.29E-6
$\ u_f - u_d\ _2$	4.77E-4	7.49E-5	8.34E-6	8.52E-7	8.55E-8	8.56E-9	8.56E-10

Noteworthy, exploiting the analytical control f_{an} as initial control for the computation of \bar{f} , the computation time can be reduced by 33% compared to random or uniform starting values even for this simple single component RD system in a relatively small space-time cylinder Q . Thus, we expect a much larger speedup of computation time for multi-component systems as well as in higher spatial dimensions.

3 Sparse Optimal Control

In applications, it might be desirable to have controls acting only in some sub-areas of the domain. Sparse optimal controls provide such solutions without any a priori knowledge of these sub-areas. They result in a natural way, since the control has the best influence in these regions to achieve a certain objective functional to be minimized.

To our knowledge, sparse optimal controls were first discussed in the context of optimal control in Ref. [33]. In that paper, an elliptic linear model was discussed. Several publications followed, investigating semi-linear elliptic equations, parabolic linear, and parabolic semi-linear equations; we refer for instance to Refs. [34–36] among others.

In this section, we follow the lines of Refs. [42, 43] and recall the most important results for the sparse optimal control of the Schlögl-model and the FitzHugh-Nagumo equation.

3.1 The Control Problem

In optimal control, sparsity is obtained by extending the objective functional J by a multiple of $j(f) := \|f\|_{L^1(Q)}$, the L^1 -norm of the control f . Therefore, recalling that $J(u_f, v_f, f) =: \mathcal{F}(f)$, we consider the problem

$$(P_{\text{sp}}) \quad \text{Min } \mathcal{F}(f) + \kappa j(f), \quad f \in \mathcal{F}_{\text{ad}}.$$

for $\kappa > 0$. The first part F of the objective functional is differentiable while the L^1 -part is not.

Our goal is not only to derive first-order optimality conditions as in the previous section but also to observe the behavior of the optimal solutions for

increasing κ and ν is tending to zero. For that task we also need to introduce second-order optimality conditions.

As before, there exists at least one locally optimal solution f to problem (P_{sp}) , denoted by \bar{f} . We refer to Ref. [42, Theorem 3.1] for more details. While \mathcal{F} is twice continuously differentiable, the second part $j(f)$ is only Lipschitz convex but not differentiable. For that reason, we need the so-called subdifferential of $j(f)$. By subdifferential calculus and using directional derivatives of $j(f)$, we are able to derive necessary optimality conditions.

3.2 First-Order Optimality Conditions

We recall some results from Refs. [42, 43]. Due to the presence of $j(f)$ in the objective functional, there exists a $\bar{\lambda} \in \partial j(\bar{f})$ such that the variational inequality Eq. (19) changes to

$$\int_0^T \int_{\Omega} d\mathbf{x} dt \{(\bar{\varphi} + \nu \bar{f} + \kappa \bar{\lambda})(f - \bar{f})\} \geq 0 \text{ for all } f \in \mathcal{F}_{\text{ad}} \cap U(\bar{f}). \quad (24)$$

For the problem (P_{sp}) , a detailed and extensive discussion of the first-order necessary optimality condition leads to very interesting conclusions, namely

$$\bar{f}(\mathbf{x}, t) = 0, \text{ if and only if } |\bar{\varphi}(\mathbf{x}, t)| \leq \kappa, \quad (25)$$

$$\bar{f}(\mathbf{x}, t) = \text{Proj}_{[u_a, u_b]} \left(-\frac{1}{\nu} [\bar{\varphi}(\mathbf{x}, t) + \kappa \bar{\lambda}(\mathbf{x}, t)] \right), \quad (26)$$

$$\bar{\lambda}(\mathbf{x}, t) = \text{Proj}_{[-1, +1]} \left(-\frac{1}{\kappa} \bar{\varphi}(\mathbf{x}, t) \right), \quad (27)$$

if $\nu > 0$. We refer to Refs. [35, Corollary 3.2] and [44, Theorem 3.1], where also the case $\nu = 0$ is discussed.

The relation in Eq. (25) leads to the sparsity of the (locally) optimal solution \bar{f} , depending on the sparsity parameter κ . In particular, the larger the choice of κ is the smaller does the support of \bar{f} become. To be more precise, there exists a value $\kappa_0 > \infty$ such that for every $\kappa \geq \kappa_0$ the only local minimum \bar{f} is equal to zero. Obvious, this case is ridiculous and thus, one needs some intuition to find a suitable value κ . We emphasize that $\bar{\lambda}$ is unique, see Eq. (27), which is important for numerical calculations.

3.3 Example 2: Optimal and Sparse Optimal Position Control

For the numerical computations, we follow the lines of Ref. [42] and use a non-linear conjugate gradient method. The advantage of using a (conjugate) gradient method lies in the simplicity in its implementation. Moreover, it allows to solve the systems Eq. (12) and the adjoint system separately. The

disadvantage is clearly the fact that it might cause a huge amount of iterations to converge, cf. Ref. [42, section 4].

Hence, we modify our approach by the use of *Model Predictive Control*. The idea is quite simple: Instead of optimizing the whole time-horizon, we only take a very small number of time steps, formulate a sub-problem and solve it. Then, the first computed time-step of the solution \bar{f} of this smaller problem is accepted on $[0, t_1]$ and is fixed. A new sub-problem is defined by going one time-step further and so on. Although the control gained in this way is only sub-optimal, it leads to a much better convergence-behavior in many computations.

Next, we revisit the task to extinguish a spiral wave by controlling its tip dynamics such that the whole pattern moves out of the spatial domain towards the Neumann boundaries [9, 21, 45]. To this goal, following Ex. 6 from Ref. [42, Section 4], we set the protocol of motion to $\phi(t) = (0, \min\{120, 1/16 t\})^T$ and $u_d(\mathbf{x}, t) := u_{\text{nat}}(\mathbf{x} - \phi(t), t)$ where u_{nat} denotes the naturally develop spiral wave solution of Eq. (12) for $f = 0$. In our numerical simulation, we take only 4 time-steps in each sub-problem of the receding horizon. Moreover, we set the kinetic parameters in the FHN model, Eq. (12), to $a = 0.005$, $\alpha = 1$, $\beta = 0.01$, $\gamma = 0.0075$, and $\delta = 0$. Further, we fix the simulation domain $\Omega = (-120, 120) \times (-120, 120)$, the terminal time $T = 2000$, $\nu = 10^{-6}$ as Tikhonov parameter, and $u_a = -5$ and $u_b = 5$ as bounds for the control, respectively. As initial state (u_0, v_0) a naturally developed spiral wave whose core is located at $(0, 0)$ is used; u_0 is presented in Fig. 2a.

In addition, an observation-function $c_d^U \in L^\infty(Q)$ instead of the constant factor $c_d^U \in \mathbb{R}$ is used, which support is only the area close to the desired spiral-tip. To be more precise, $c_d^U(\mathbf{x}, t) = 1$ in the co-moving area defined by all $(\mathbf{x}, t) \in Q$ such that $|\mathbf{x} - \bar{\mathbf{x}}(t)| \leq 20$ and vanishes identically otherwise. The other coefficients c_d^V , c_T^U , and c_T^V are set equal to zero.

The reason for the choice of such an observation-function is clear: a most intriguing property of spiral waves is that despite being propagating waves affecting all accessible space, they behave as effectively localized particles-like objects [46]. The particle-like behavior of spirals corresponds to an effective localization of so called *response functions* [47, 48]. The asymptotical theory of the spiral wave drift [49] is based on the idea of summation of elementary responses of the spiral wave core position and rotation phase to elementary perturbations of different modalities and at different times and places. This is mathematically expressed in terms of the response functions must decay quickly with distance from the spiral wave core and are equal to zero in the region where the spiral wave is insensitive to small perturbations.

The numerical results for the sup-optimal control ($\kappa = 0$) and for the sparse sub-optimal control ($\kappa = 1$) are depicted in Fig. 2b and Fig. 2c, respectively. One notices that the prescribed spiral tip trajectory is realized for both choices for the sparsity parameter κ , viz., $\kappa = 0$ and $\kappa = 1$. The traces of the spiral tip is indicated by the solid lines in both panels. Since the spiral tip

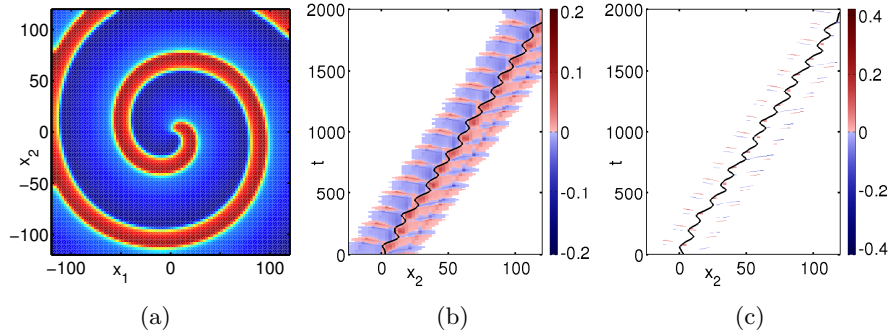


Fig. 2. (a) Spiral wave solution to Eq. (12) with $\mathbf{f} = 0$ is used as initial state in the problem (P_{SP}). (b) Numerically obtained sub-optimal control ($\kappa = 0$) and (c) sparse sub-optimal control solution ($\kappa = 1$), both shown in the x_2 - t -plane for $x_1 = 0$ with associated spiral-tip trajectory (black line). The magnitude of the control signal is color-coded. The remaining system parameters are $a = 0.005$, $\alpha = 1$, $\beta = 0.01$, $\gamma = 0.0075$, and $\delta = 0$. In the optimal control algorithms, we set $\nu = 10^{-6}$, $u_a = -5$, and $u_b = 5$.

rotates rigidly around the spiral core which moves itself on a straight line according to $\phi(t)$, one observes a periodic motion of the tip in the x_2 - t -plane. In addition, the area of non-zero control (colored areas) is obviously much smaller for non-zero sparsity parameter κ compared to the case $\kappa = 0$, cf. Fig. 2b and Fig. 2c. However, the amplitude of the sparse control is two times larger.

3.4 Second-Order Optimality Conditions and Numerical Stability

To avoid this subsection to become too technical, we only state the main results from Ref. [43]. We know for an unconstrained problem with differentiable objective-functional that it is sufficient to show $F'(\bar{f}) = 0$ and $F''(\bar{f}) > 0$ to derive that \bar{f} is a local minimizer of F , if F were a real-valued function of one real variable. More details about the importance of second order optimality conditions in the context of PDE control can be found in Ref. [50].

In our setting, considering all directions $h \neq 0$ out of a certain so-called critical cone C_f , the condition for $\nu > 0$ reads

$$F''(\bar{f})h^2 > 0.$$

Then, \bar{f} is a locally optimal solution of (P_{SP}). The detailed structure of C_f is described in Ref. [43]; also the much more complicated case $\nu = 0$ is discussed there.

The second-order sufficient optimality conditions are the base for observing interesting questions. For example, the stability of solutions for perturbed

desired trajectories and desired states is discussed [43]. Moreover, we study the limiting case of Tikhonov parameter ν tending to zero.

3.5 Tikhonov parameter tending to zero

In this section, we investigate the behavior of a sequence of optimal controls and the corresponding states as solutions of the problem (P_{sp}) as $\nu \rightarrow 0$. For this reason, we denote our control problem (P_ν) , the associated optimal control with \bar{f}_ν , and its associated states with $(\bar{u}_\nu, \bar{v}_\nu)$ for a fixed $\nu \geq 0$. Since \mathcal{F}_{ad} is bounded in $L^\infty(Q)$, any sequence of solutions $\{\bar{f}_\nu\}_{\nu>0}$ of (P_ν) has subsequences converging weakly* in $L^\infty(Q)$. For a direct numerical approach, this is useless but with second order sufficient optimality conditions we can deduce interesting consequences of this convergence.

Assume that the second order sufficient optimality conditions of Ref. [43, Theorem 4.7] are satisfied. Then, with $(\bar{u}_\nu, \bar{v}_\nu) = G(\bar{f}_\nu)$ and $(\bar{u}_0, \bar{v}_0) = G(\bar{f}_0)$, we derive a Hölder rate of convergence for the states

$$\lim_{\nu \rightarrow 0} \frac{1}{\sqrt{\nu}} \{ \|\bar{u}_\nu - \bar{u}_0\|_{L^2(Q)} + \|\bar{v}_\nu - \bar{v}_0\|_{L^2(Q)} \} = 0. \quad (28)$$

We should mention that this estimate is fairly pessimistic. All of our numerical tests show that the convergence rate is of order ν , i.e., numerically, we see a Lipschitz rather than a Hölder estimate [43]. As mentioned in Ref. [43], it should also be possible to prove Lipschitz stability with a remarkable amount of effort and hence, to confirm the linear rate of convergence for $\nu \rightarrow 0$.

3.6 Example 3: Sparse Optimal Control with Tikhonov parameter tending to zero

Finally, we consider a traveling pulse solution in the FitzHugh-Nagumo system in one spatial dimension $N = 1$. Here, the limiting case of vanishing Tikhonov parameter, $\nu = 0$, is of our special interest. We observe that Newton-type methods can be used with very high accuracy even for very small values of $\nu > 0$. This allows us to study the convergence behavior of solutions for ν tending to zero as well.

Following Ref. [43] and in contrast to the last example in Sect. 3.3, we solve the full forward-backward-system of optimality. We stress that this is numerically solely possible for non-vanishing value of ν . However, we constructed examples where an exact solution of the optimality system for $\nu = 0$ is accessible as shown in Ref. [43, Section 5.3]. In this sequel, our reference-solution, denoted by \bar{u}_{ref} , will be the solution of (P_ν) for $\nu = 10^{-10}$.

Next, we treat the well-studied problem of pulse nucleation [51, 52] by sparse optimal control. We aim to start and to stay in the lower homogeneous steady state (HSS) for the first two time-units, i.e., $u_d(\mathbf{x}, t) = -1.3$ for $t \in (0, 2)$. Then, the state shall jump instantaneously into traveling pulse solution

u_{nat} , i.e., $u_d(\mathbf{x}, t) = u_{\text{nat}}(\mathbf{x}, t - 2)$. To get a solution u_{nat} , we solve Eq. (12) for $f = 0$ and a suitable initial state as shown in Fig. 3a.

In our optimal control algorithms, we set the parameters to $\Omega = (0, 75)$, $T = 10$, $\alpha = 1$, $\beta = 0$, $\gamma = 0.33$, and $\delta = -0.429$. Moreover, we use a slightly different nonlinear reaction kinetics $R(u) = u(u - \sqrt{3})(u + \sqrt{3})$ in Eq. (12) but this does not change the analytical results. The upper and lower bounds for the control f are set to very large values, viz. $u_a = -100$ and $u_b = 100$. In addition, the coefficients in Eq. (13) are kept fixed, viz., $c_d^U = 1$ and $c_T^U = c_d^V = c_T^V = 0$.

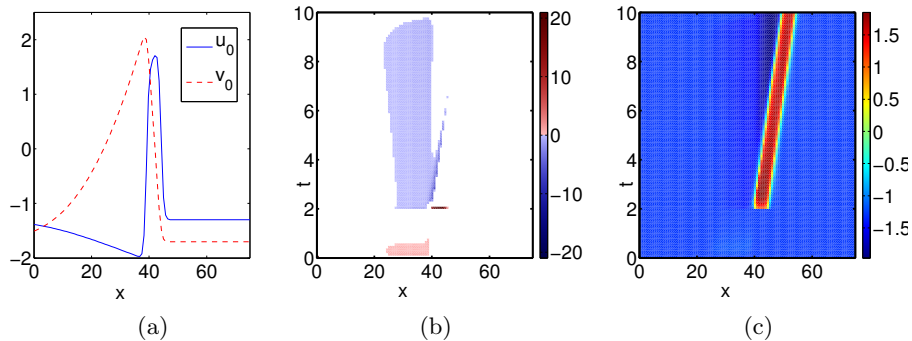


Fig. 3. (a) Segment of a traveling impulse solution $(u_0, v_0)^T$ in the uncontrolled FitzHugh-Nagumo system, Eq. (12). (b) Numerically obtained sparse optimal control solution \bar{f}_ν for almost vanishing Tikhonov parameter, $\nu = 10^{-10}$, and (c) the associated optimal state \bar{u}_ν . The magnitude of the control signal is color-coded. The kinetic parameter values are set to $\alpha = 1$, $\beta = 0$, $\gamma = 0.33$, $\delta = -0.429$, and $R(u) = u(u - \sqrt{3})(u + \sqrt{3})$.

Our numerical results obtained for a sparse optimal control \bar{f}_ν acting solely on the activator u , cf. Eq. (12), are presented in Fig. 3b and Fig. 3c. In order to create a traveling pulse solution from the HSS $u_d = -1.3$, the optimal control resembles a step-like excitation at $x \simeq 40$ with a very high amplitude. Since the Tikhonov parameter is set to $\nu = 10^{-10}$, large control amplitudes are to be expected and indicate that in the unregularized case, even a delta distribution might appear. Because this excitation is supercritical a new pulse will nucleate. In order to inhibit the propagation of this nucleated pulse to the left, the control must act at the back of the pulse as well. Thus, we observe a negative control amplitude acting in the back of the traveling pulse. We emphasize that the desired shape of the pulse is achieved qualitatively. The realization of the exact desired profile can not be expected due to a not large but noticeable sparse parameter $\kappa = 0.01$. Even for this respectively small value, the sparsity of the optimal control shows.

Since the displayed control and state are computed for an almost vanishing value $\nu = 10^{-10}$, we take the associated state as reference-state \bar{u}_{ref} to compare

the difference $\|\bar{u}_\nu - \bar{u}_{\text{ref}}\|_{L^2(Q)}$ for decreasing values $\nu > 0$. From Table 2, one notices the already mentioned Lipschitz-rate of convergence for decreasing values $\nu > 0$, $\|\bar{u}_\nu - \bar{u}_{\text{ref}}\|_{L^2(Q)} \propto \nu^{-1}$. This observation is consistent to results from [43] for various other examples.

Table 2. The comparison of the distance $\|\bar{u}_\nu - \bar{u}_{\text{ref}}\|_{L^2(Q)}$ between the numerically obtained states \bar{u}_ν and the numerically obtained reference-solution \bar{u}_{ref} , computed for $\nu = 10^{-10}$, for decreasing values of $\nu > 0$.

ν	1E-3	1E-4	1E-5	1E-6	1E-7	1E-8	1E-9
$\ \bar{u}_\nu - \bar{u}_{\text{ref}}\ _{L^2(Q)}$	1.58E-1	1.16E-2	1.33E-3	1.35E-4	1.35E-5	1.34E-6	1.31E-7

4 Conclusion

Optimal control of traveling waves according to a given desired distribution is important for many applications.

Analytical solutions to this control problem can be obtained with ease from (8) discussed in Sect. 2. Furthermore, in case of position control, the analytical solution can be obtained without full information about the underlying nonlinear reaction kinetics. Moreover, the analytical expressions for the control solve the corresponding unregularized optimal control problem. Therefore, they are a good starting point for the numerical solution of the regularized optimal position control problem, Sect. 2. The numerical computation of the optimal control for the position of front and pulse solutions to the Schlögl and FitzHugh-Nagumo equations, for example, is speed-up substantially. Generally, the analytical expressions may serve as consistency check for numerical algorithms in optimal control.

As expected, the control signal is spatially localized in position control of fronts, pulses and spiral waves. Applying sparse optimal position control, Sect. 3, the size of the domains where the control acts can be further decreased. Importantly, the method determines sparse controls without any a priori knowledge about restrictions to certain subdomains. Additionally, sparse control allows to study second order optimality conditions that are not only interesting from the theoretical perspective but also for numerical Newton-type algorithms.

References

1. F. Schlögl, Z. Phys. **253**, 147 (1972)
2. A. Winfree, Science **175**, 634 (1972)
3. J.J. Tyson, J.P. Keener, Physica D: Nonlinear Phenomena **32**(3), 327 (1988)

4. R. Kapral, K. Showalter (eds.). *Chemical Waves and Patterns* (Kluwer, Dordrecht, 1995)
5. Y. Kuramoto, *Chemical Oscillations, Waves, and Turbulence* (Courier Dover Publications, New York, 2003)
6. J. Murray, *Mathematical Biology* (Springer-Verlag, Berlin, 2003)
7. A. Liehr, *Dissipative solitons in reaction diffusion systems: Mechanisms, dynamics, interaction*, vol. 70 (Springer Science & Business Media, 2013)
8. V.S. Zykov, G. Bordiougov, H. Brandtstädter, I. Gerdes, H. Engel, Phys. Rev. Lett. **92**, 018304 (2004)
9. V.S. Zykov, H. Engel, Physica D **199**, 243 (2004)
10. A. Mikhailov, K. Showalter, Phys. Rep. **425**, 79 (2006)
11. J. Schlesner, V.S. Zykov, H. Engel, E. Schöll, Phys. Rev. E **74**, 046215 (2006)
12. M. Kim, M. Bertram, M. Pollmann, A. von Oertzen, A.S. Mikhailov, H.H. Rotermund, G. Ertl, Science **292**, 1357 (2001)
13. V.S. Zykov, G. Bordiougov, H. Brandtstädter, I. Gerdes, H. Engel, Phys. Rev. E **68**, 016214 (2003)
14. J.X. Chen, H. Zhang, Y.Q. Li, J. Chem. Phys. **130**(12), 124510 (2009)
15. H.W. Engl, T. Langthaler, P. Mansellio, in *Optimal control of partial differential equations*, ed. by K.H. Hoffmann, W. Krabs (Birkhäuser Verlag, Basel, 1987), pp. 67–90
16. W. Barthel, C. John, F. Tröltzsch, To appear in Z. Angew. Math. und Mech. (DOI: 10.1002/zamm.200900359)
17. R. Buchholz, H. Engel, E. Kammann, F. Tröltzsch, Comput. Optim. Appl. **56**, 153 (2013)
18. G. Haas, M. Bär, I.G. Kevrekidis, P.B. Rasmussen, H.H. Rotermund, G. Ertl, Phys. Rev. Lett. **75**, 3560 (1995)
19. S. Martens, J. Löber, H. Engel, Phys. Rev. E **91**, 022902 (2015)
20. V.S. Zykov, H. Brandtstädter, G. Bordiougov, H. Engel, Phys. Rev. E **72**(R), 065201 (2005)
21. O. Steinbock, V.S. Zykov, S.C. Müller, Nature **366**(6453), 322 (1993)
22. A. Schrader, M. Braune, H. Engel, Phys. Rev. E **52**, 98 (1995)
23. T. Sakurai, E. Mihaliuk, F. Chirila, K. Showalter, Science **296**(5575), 2009 (2002)
24. J. Wolff, A.G. Papathanasiou, H.H. Rotermund, G. Ertl, X. Li, I.G. Kevrekidis, Phys. Rev. Lett. **90**, 018302 (2003)
25. J. Wolff, A.G. Papathanasiou, I.G. Kevrekidis, H.H. Rotermund, G. Ertl, Science **294**(5540), 134 (2001)
26. B.A. Malomed, D.J. Frantzeskakis, H.E. Nistazakis, A.N. Yannacopoulos, P.G. Kevrekidis, Phys. Lett. A **295**, 267 (2002)
27. P.G. Kevrekidis, I.G. Kevrekidis, B.A. Malomed, H.E. Nistazakis, D.J. Frantzeskakis, Phys. Scr. **69**, 451 (2004)
28. J. Löber, H. Engel, Phys. Rev. Lett. **112**, 148305 (2014)
29. J. Löber, Phys. Rev. E **89**, 062904 (2014)
30. J. Löber, R. Coles, J. Siebert, H. Engel, E. Schöll, in *Engineering of Chemical Complexity II*, ed. by A. Mikhailov, G. Ertl (World Scientific, Singapore, 2015)
31. J. Löber, S. Martens, H. Engel, Phys. Rev. E **90**, 062911 (2014)
32. K.H. Hoffmann, G. Leugering, F. Tröltzsch (eds.), *Optimal Control of Partial Differential Equations, ISNM*, vol. 133 (Birkhäuser Verlag, 1998)
33. G. Stadler, Comput. Optim. Appl. **44**, 159 (2009)

34. G. Wachsmuth, D. Wachsmuth, ESAIM Control Optim. Calc. Var. **17**(3), 858 (2011)
35. E. Casas, R. Herzog, G. Wachsmuth, SIAM J. Optim. **22**(3), 795 (2012)
36. E. Casas, F. Tröltzsch, SIAM J. Control Optim. **52**, 1010 (2014)
37. A. Azhand, J.F. Tötz, H. Engel, Eur. Phys. Lett. **108**, 10004 (2014)
38. J. Löber, Optimal trajectory tracking. Ph.D. thesis, TU Berlin (2015)
39. J. Nagumo, Proc. IRE **50**, 2061 (1962)
40. R. FitzHugh, Biophys. Journal **1**, 445 (1961)
41. Y. Zeldovich, D. Frank-Kamenetsky, Dokl. Akad. Nauk SSSR **19**, 693 (1938)
42. E. Casas, C. Ryll, F. Tröltzsch, Computational Methods in Applied Mathematics **13**, 415 (2013)
43. E. Casas, C. Ryll, F. Tröltzsch, SIAM J. Control Optim.
44. E. Casas, SIAM J. Control Optim. **50**, 2355 (2012)
45. J. Schlesner, V.S. Zykov, H. Brandtstädter, I. Gerdes, H. Engel, New J. Phys. **10**, 015003 (2008)
46. I.V. Biktasheva, V.N. Biktashev, Phys. Rev. E **67**, 026221 (2003)
47. H. Henry, V. Hakim, Phys. Rev. E **65**, 046235 (2002)
48. I.V. Biktasheva, D. Barkley, V.N. Biktashev, A.J. Foulkes, Phys. Rev. E **81**, 066202 (2010)
49. J.P. Keener, Physica D **31**, 269 (1988)
50. E. Casas, F. Tröltzsch, Jahresbericht der Deutschen Mathematiker-Vereinigung (2014)
51. A. Mikhailov, L. Schimansky-Geier, W. Ebeling, Phys. Lett. A **96**(9), 453 (1983)
52. I. Idris, V.N. Biktashev, Phys. Rev. Lett. **101**, 244101 (2008)